A Small-Scale Fading Model for Overtaking Vehicles in a Millimeter Wave Communication Link

Erich Zöchmann*†‡, Herbert Groll†, Stefan Pratschner*†

* Christian Doppler Laboratory for Dependable Wireless Connectivity for the Society in Motion,
† Institute of Telecommunications, TU Wien, Austria *ezoechma@nt.tuwien.ac.at*
‡ Department of Radio Electronics, TU Brno, Czech Republic

***Abstract*—We derive a small-scale fading model for the typical situation of cars driving on parallel lanes. The small-scale fading for an overtaking vehicle appearing in the inter-vehicle millimeter wave communication link is modeled as two-wave with diffuse power (TWDP) fading. The evolution of the TWDP parameters follows a first-order linear differential equation. A main parameter of the solution function of this differential equation is the effective length of the overtaking vehicle. This length matches fairly well the spatial extend of the overtaking vehicles.**

***Index Terms*—TWDP fading, millimeter wave, moving scattering objects**

I. Introduction

Wireless communication using millimeter waves (mmWaves) has been a focus of research for more than four decades [1]. The potential of having broadband channels and highly directive beams have attracted attempts for the employment of mmWaves in vehicular communication [2]. Although frequency bands at mmWave have been allocated for intelligent transport systems (ITS) since at least the 1990s [3], their deployment is scarce and has been proven challenging so far. The recent interest in autonomous driving and the need for higher bandwidth have revived research in mmWave vehicular communication [4]. Key results of early narrowband vehicle-to-vehicle (V2V) mmWave measurements, such as [5]–[10], are summarized in [2]. For example, outage probability of vehicle-to-infrastructure (V2I) mmWave channels is analyzed in [5], V2V and V2I mmWave broadband communication is considered in [6], and in [10] path-loss predictions models for line of sight (LOS) and non-line of sight (NLOS) communication from measurements of a V2V scenario at 60 GHz are derived. More recently, the properties of V2V and V2I communication channels for broadband mmWave have been investigated in several measurement campaigns [12]–[19]. An attempt to model the time-varying channel for mmWave railway communication with reasonable complexity employs ray-tracing [11]. While there are no other surrounding, moving objects in the railway environment, the urban vehicular environment is much more complex and thus the wireless channel is much more difficult to model, prohibiting the usage of ray-tracing. The directional antennas have an impact on the temporal variation of the mmWave channel [12]. V2I measurements in expressway environments are shown in [13] for 28 GHz in form of Doppler profiles and in [14] for 60 GHz in terms of power delay profiles. V2V mmWave channels in terms of blockage are measured in [16] simultaneously with additional frequency bands. Measurements with a focus on the effect of overtaking or passing cars on V2V channels at 60 GHz are shown in [17], [18]. The statistical evaluation of overtaking vehicles for such V2V channels is provided in [20].

The two-wave with diffuse power (TWDP) model to describe small-scale fading is first presented in [21]. MmWave Measurements showing agreement with TWDP fading are shown in [22]–[27]. In our opinion, there is a lack of mmWave channel models for vehicular scenarios; this hampers research and successful application of mmWave in ITS. Therefore, further mmWave fading models are a necessary resource.

Contribution: In this paper, we derive a small-scale fading model for the typical situation of communicating cars driving on parallel lanes. The presented small-scale fading model for moving scattering objects appearing in a mmWave communication link (channel) has a good fit, allows physical interpretation, and has low complexity. The analysis is carried out under the framework of TWDP fading and the evolution of its model parameters.

II. Measured Scenario

A detailed description of the 60 GHz measurement campaign and the measurement setup is found in [26]. To the benefit of the reader, we briefly summarize the campaign below. To achieve very accurate frequency and time synchronization, we keep transmitter (TX) (a tripod) and receiver (RX) (a car, marked as blue car in Fig. 1) static and connected both

The financial support by the Austrian Federal Ministry for Digital and Economic Affairs and the National Foundation for Research, Technology and Development is gratefully acknowledged. The research described in this paper was co-financed by the Czech Science Foundation, Project No. 17-27068S and 17-18675S, and by National Sustainability Program under grant LO1401. For the research, the infrastructure of the SIX Center was used. This work was carried out in the framework of COST Action CA15104 IRACON.

with a 10 MHz frequency reference and a trigger cable, see Fig. 1. The sample rate at the receiver is 600 MSamples/s. We employ a multi-tone sequence with 121 carriers to approximately achieve a tone spacing of 5 MHz. Due to the anti-aliasing filter, we avoid the cut-off region and only transmit the sounding sequence at the 101 center tones. Thereby, an effective sounding bandwidth of 510 MHz is achieved. The output of our channel sounder is the calibrated time-variant transfer function $H(t, f)$.

To obtain time-variant vehicular channels, we let urban street traffic pass by, illustrated by the green car in Fig. 1. This effectively emulates a platooning scenario, where a car platoon is being overtaken. A measurement is triggered once an overtaking vehicle of the urban street traffic drives through a light barrier. Through a second light barrier the mean velocity and the overtaking car's position at any time is estimated. We measured different overtaking vehicle types, such as passenger cars, sports utility vehicles (SUVs), and trucks.

In this contribution we are especially interested in the fading behavior of the LOS component. We obtain the LOS component by transferring the time-variant transfer function $H(t, f)$ to the time-variant channel impulse response $h(t, \tau)$, via a discrete Fourier transformation. Then we identify and select the LOS tap, τ_{LOS}, and exclusively focus on the behavior of $h(t, \tau_{\text{LOS}})$. A system bandwidth of 510 MHz provides a time resolution of approximately 2 ns and hence resolves paths which differ approximately 60 cm in path length. This condition is illustrated through a Fresnel ellipsoid in Fig. 1. The semi-minor axis of this ellipsoid is calculated through $\sqrt{\left(\frac{15\,\text{m}}{2} + \frac{60\,\text{cm}}{2}\right)^2 - \left(\frac{15\,\text{m}}{2}\right)^2} \approx 2.1\,\text{m}$. Every path with less separation is not resolved and amounts to fading.

III. Modeling Approach

TWDP fading captures the effect of interference of two non-fluctuating radio signals and many smaller so-called diffuse signals [21]. For our scenario, the two non-fluctuating signals consist of the unblocked LOS path and a scattered path from the overtaking vehicle. The TWDP distribution degenerates to the Rice distribution, if one of the two non-fluctuating radio signals vanishes. This condition is analogous to the well-known Rice degeneration to the Rayleigh distribution with decreasing K-factor. The PDF, CDF, and MGF of TWDP fading are found in [28].

The TWDP fading model in the complex-valued baseband is given as

$$r_{\text{complex}} = V_1 e^{\mathrm{j}\phi_1} + V_2 e^{\mathrm{j}\phi_2} + X + jY \ , \tag{1}$$

where $V_1 > 0$ and $V_2 \geq 0$ are the deterministic amplitudes of the non-fluctuating components. The phases ϕ_1 and ϕ_2 are independent and uniformly distributed in $(0, 2\pi)$. The diffuse components are modeled via the law of large numbers as $X + jY$, where $X, Y \sim \mathcal{N}(0, \sigma^2)$. The second moment of the envelope $r = |r_{\text{complex}}|$ of TWDP fading is given as

$$\mathbb{E}\{r^2\} = \Omega = V_1^2 + V_2^2 + 2\sigma^2 \ . \tag{2}$$

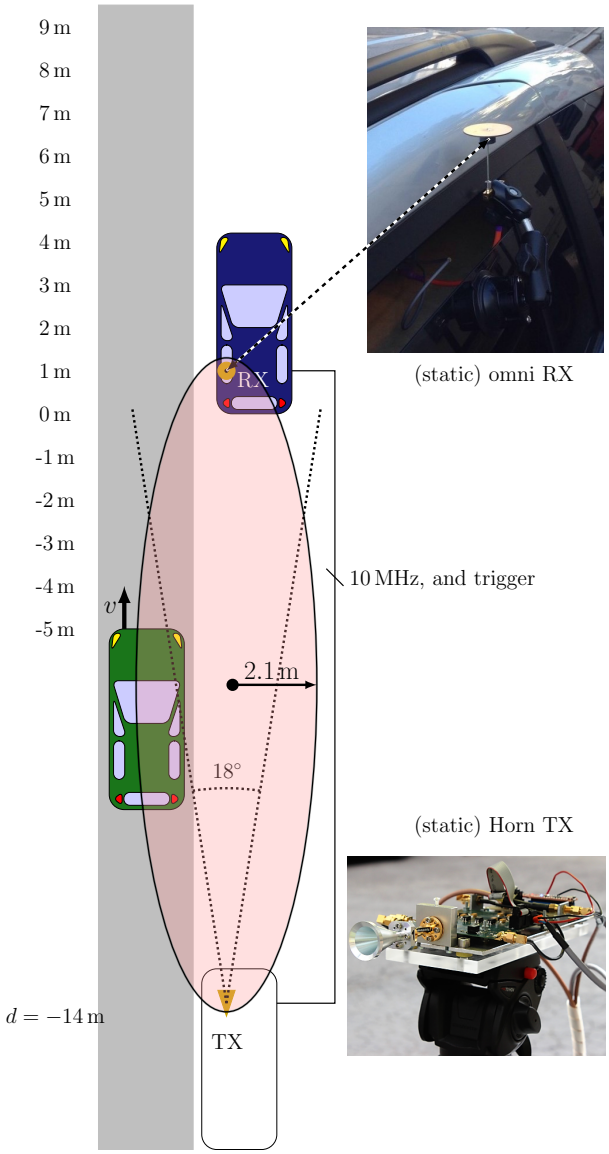

Fig. 1. Measured scenario drawn to scale. TX and RX are static to achieve good time and frequency synchronization. Urban street traffic is passing by and act as moving scattering objects. All scattering objects within the red ellipse cause paths which are not further resolved in time and thus appear at the LOS tap.

Expectation is denoted by $\mathbb{E}\{\cdot\}$. By enforcing

$$\Omega \equiv 1 \ , \tag{3}$$

all distributions are parameterized solely by the tuple (K, Δ), of which the K-factor is the power ratio of the specular (non-fluctuating) components to the diffuse components

$$K = \frac{V_1^2 + V_2^2}{2\sigma^2} \ . \tag{4}$$

The parameter Δ describes the amplitude relationship among the specular components

$$\Delta = \frac{2V_1V_2}{V_1^2 + V_2^2} \ . \tag{5}$$

The Δ-parameter is bounded between 0 and 1, and equals 1 if, and only if, both amplitudes are equal. By combining Eq. (2), (3), and (4) the second moment of the diffuse components equals to

$$\sigma^2 = \frac{1}{2\,(1+K)}\ . \tag{6}$$

A LASSO [29], [30] based sparsity analysis revealed that our measured channel is dominated by the LOS component, a more than 10 dB weaker component of the overtaking vehicle and a few smaller background components [31]–[33]. Hence, as mentioned, given the measured channel impulse responses (CIRs) during the overtaking process, we select the LOS tap and focus on its amplitude fading distribution. To obtain the parameter tuple (K, Δ), the method of maximum likelihood estimation is employed [25], [26].

One parameter tuple describes the fading condition on a segment of $50\lambda = 0.25$ m. A passing vehicle has an effect such that the parameter tuple changes and saturates as the distance increases. Due to the spatial extend of the vehicle, a smooth transition can be expected. The K-factor that appears without a vehicle present is denoted as $K_{d\to\infty}$. This constant is chosen to be $K_{d\to\infty} = 46$ dB, since this is the highest observed value. The K-factor change (in dB) is modeled through the first-order linear differential equation

$$\frac{\partial K(d)}{\partial d} = \frac{\big(K_{d\to\infty} - K(d)\big)}{\delta}, \qquad K(0) = (1-\kappa)\,K_{d\to\infty}\ . \tag{7}$$

The parameter δ acts as effective length of the overtaking vehicle. The larger δ, the slower the change of K. Furthermore, if there is a large deviation from $K_{d\to\infty}$, a vehicle is very close to the RX antenna. Hence, the K-factor should be able to change faster. The measured data show a symmetry around $d = 0$. The solution which incorporates symmetry around $d = 0$ is given by

$$K(d) = K_{d\to\infty}\left(1 - \kappa \exp\left(-\frac{|d|}{\delta}\right)\right)\ . \tag{8}$$

The factor κ models the maximum reduction of the K-factor when a vehicle is present.

Likewise, the Δ-parameter is modeled to fulfill

$$\frac{\partial \Delta(d)}{\partial d} = -\frac{\Delta(d)}{\delta}, \qquad \Delta(0) = \Delta_{\text{max}}\ . \tag{9}$$

Again, the solution is a symmetric exponential function

$$\Delta(d) = \Delta_{\text{max}} \exp\left(-\frac{|d|}{\delta}\right)\ , \tag{10}$$

where Δ_{max} models the strongest reflection from the overtaking vehicle. Here, the δ-parameter has the same meaning as for the K-factor. We distinguish between a joint and an individual δ for fitting of K and Δ later on.

Why is the K-factor modeled in logarithmic and the Δ-parameter in linear scale?: Through our previous analysis [31]–[33] we conclude that $V_2 \ll V_1$, and hence $\Delta \approx {}^{2V_2}/_{V_1}$. As V_1 is the amplitude of the unblocked LOS component, it is constant during the measurements. Thus, Δ is proportional to the *amplitude* of the scattered component, i.e., $\Delta \propto V_2$. Contrary, $K \approx {}^{V_1^2}/_{(2\sigma^2)}$, and, again, as V_1 stays constant, the change of K is due to a *power* change of the diffuse components. Hence, we want to model the behavior of the "amplitudes" $\sigma \propto K^{-1/2}$ via a linear differential equation. The nonlinear transform of the inverse square root (mainly its concavity) is captured well by the concavity of the $-\log$ curve.

IV. Results

Given the ansatz functions developed in the section above, we perform a least-squares fit with the ML fitted parameter tuple to obtain the model parameters. Principally, the δ parameter in Eqs. (8) and (10) models the effective length of the overtaking vehicle. As such, this parameter should be the same in both equations. An individual δ parameter in each equation allows, however, a better fit. We will compare two competing strategies in the following.

For the individual fit of the K-factor and the Δ-parameter models, MATLAB's nonlinear least-square fitting tool was utilized. Scatter plots of the observed K-factor, distinguished by vehicle type, are shown in Fig. 2 left-hand side. Scatter plots of the corresponding Δ-parameter are shown right-hand side. The individual fits of the K-factor model (8) and the Δ-parameter model (10) are shown in black dashed lines. The individually fitted model parameters are annotated in the lower left corner of the K-factor panels and in the upper right corner of the Δ-parameter panels.

For the joint fit, we employ the following strategy. Firstly, we linearize the ansatz functions (8) and (10) via a natural logarithm transform. We thereby achieve the following equations.

$$\begin{aligned} \log\left(1 - \frac{K(d)}{K_{d\to\infty}}\right) &= \log\kappa \qquad\quad - \frac{1}{\delta}|d| \\ \log\Delta(d) &= \log\Delta_{\text{max}} \quad - \frac{1}{\delta}|d| \end{aligned} \tag{11}$$

Through stacking all equations from the first distance d_1 until the last distance d_N, we achieve the following matrix-vector equation

$$\begin{bmatrix} \log\left(1 - \frac{K(d_1)}{K_{d\to\infty}}\right) \\ \vdots \\ \log\left(1 - \frac{K(d_N)}{K_{d\to\infty}}\right) \\ \hdashline \log\Delta(d_1) \\ \vdots \\ \log\Delta(d_N) \end{bmatrix} = \left[\begin{array}{ccc} 1 & 0 & -|d_1| \\ \vdots & \vdots & \vdots \\ 1 & 0 & -|d_N| \\ \hdashline 0 & 1 & -|d_1| \\ \vdots & \vdots & \vdots \\ 0 & 1 & -|d_N| \end{array}\right] \begin{bmatrix} \log\kappa \\ \log\Delta_{\text{max}} \\ \frac{1}{\delta} \end{bmatrix}\ . \tag{12}$$

By applying the Moore-Penrose inverse to (12), the solution parameters are found.

As mentioned earlier, the joint parameter fit avoids the ambiguous δ-parameter, as this parameter is common for the parameter tuple. This approach, however, comes with the disadvantage that some observations need to be withdrawn

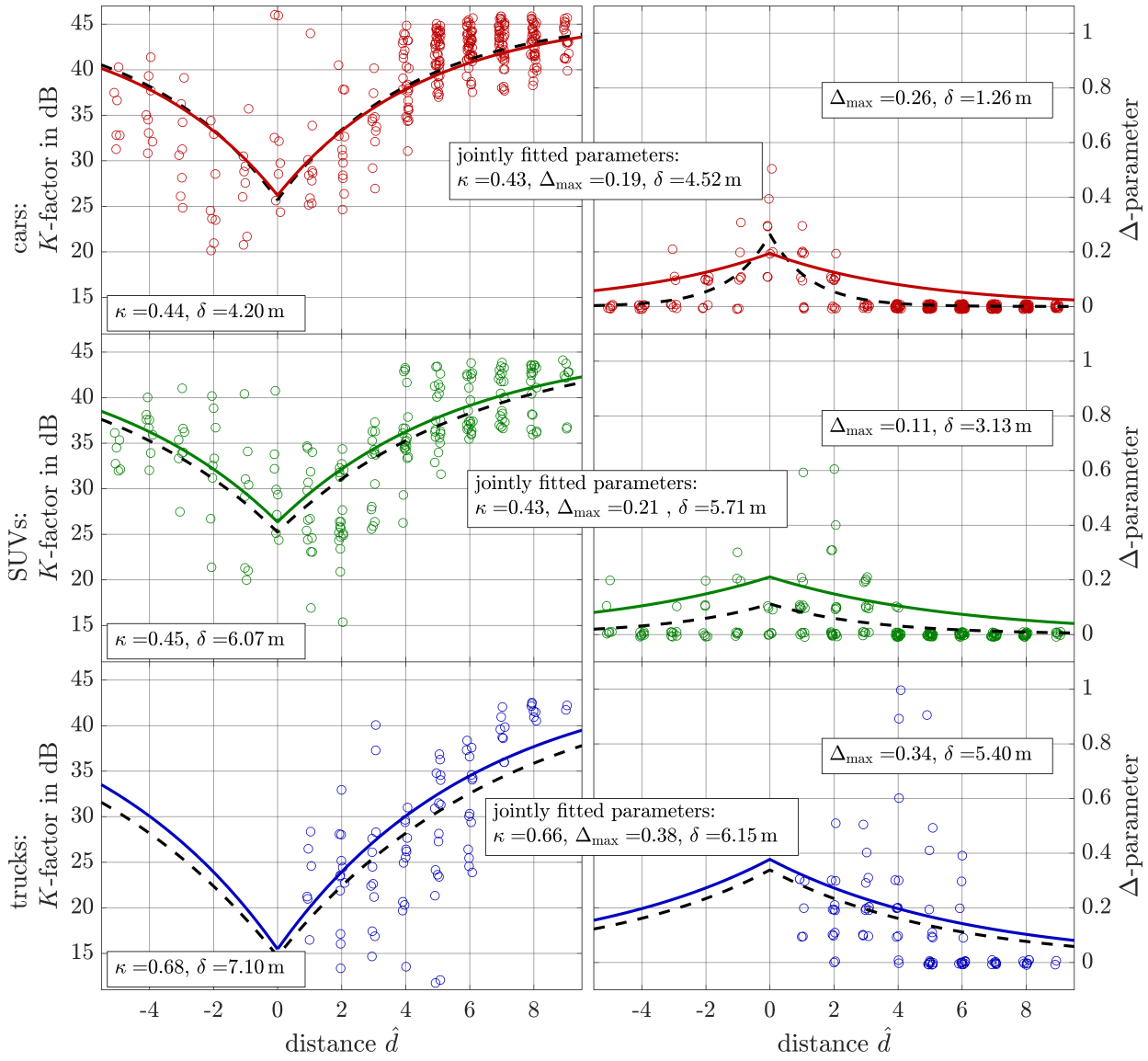

Fig. 2. Effective vehicle length estimation through exponential modeling of the parameter tuple. (Left) The fitted K-factors for cars, SUVs, and trucks are shown from top to bottom. (Right) The fitted Δ-parameters for cars, SUVs, and trucks are also shown from top to bottom. The effective lengths range from $\delta \in (1.26\,\text{m}, 7.1\,\text{m})$. The effective length δ scales with the vehicle length. The joint fits in solid lines show a disagreement for the Δ-parameters. As the joint fit evokes the logarithm transform, we did not use Δ values close to 0 and hence biased the fit.

from the data set, as values close to 0 are problematic in the logarithm term of the left-hand side in (12). In this contribution, we skip those observations with the logarithm argument smaller than 0.1 .

The joint least-squares fit of the parameters is plotted in Fig. 2 as solid lines. The fitted model parameters are plotted across the corresponding panels. The effective length is between 4.52 m and 6.15 m, and hence matches fairly well the vehicle lengths. In the case of an individual K-factor fit, the effective length is similar and between 4.2 m and 7.1 m. In contrast, when Δ-parameter is fitted individually, the effective lengths are smaller and range from 1.3 to 5.4 m. The maximum reduction of the K-factor is between 43% and 66% and the maximum Δ-parameters fall between 0.19 and 0.38.

V. Conclusion

We model the effect of overtaking interacting objects (vehicles) on a millimeter wave inter-vehicle communications link. For 500 MHz bandwidth the scattered component of the overtaking vehicle appears at the LOS tap and fading according to a TWDP statistic is observed. The parameters of the TWDP model change continuously as the overtaking vehicle passes by. The continuity is well modeled via a first-order linear differential equation. We show individual fits for the K-factor and the Δ-parameter, as well as a joint fit. The solution function contains the import parameter of effective vehicle length δ, which matches the physical length of the overtaking vehicle fairly well. The other parameters are the K-factor reduction factor which is around $\kappa \approx 0.5$. The final

parameter is the maximum Δ-parameter which was observed to be approximately $\Delta_{\max} \approx 0.4$ for trucks.

REFERENCES

[1] H. H. Meinel, "Commercial applications of millimeterwaves: history, present status, and future trends," *IEEE Transactions on Microwave Theory and Techniques*, vol. 43, no. 7, pp. 1639–1653, 1995.

[2] V. Va, T. Shimizu, G. Bansal, and R. W. Heath Jr, "Millimeter wave vehicular communications: A survey," *Foundations and Trends® in Networking*, vol. 10, no. 1, pp. 1–113, 2016.

[3] H. Meinel, "Applications of microwaves and millimeterwaves for vehicle communications and control in europe," *Proc. of IEEE MTT-S Microwave Symposium*, pp. 609–612, 1992.

[4] J. Choi, V. Va, N. Gonzalez-Prelcic, R. Daniels, C. R. Bhat, and R. W. Heath Jr., "Millimeter-wave vehicular communication to support massive automotive sensing," *IEEE Communications Magazine*, vol. 54, no. 12, pp. 160–167, 2016.

[5] R. Verdone, "Outage probability analysis for short-range communication systems at 60 GHz in ATT urban environments," *IEEE Transactions on Vehicular Technology*, vol. 46, no. 4, pp. 1027–1039, 1997.

[6] O. Andrisano, V. Tralli, and R. Verdone, "Millimeter waves for short-range multimedia communication systems," *Proceedings of the IEEE*, vol. 86, no. 7, pp. 1383–1401, 1998.

[7] R. Schneider, D. Didascalou, and W. Wiesbeck, "Impact of road surfaces on millimeter-wave propagation," *IEEE Transactions on Vehicular Technology*, vol. 49, no. 4, pp. 1314–1320, 2000.

[8] K. Akihito, S. Katsuyoshi, M. Fujise, and S. Kawakami, "Propagation characteristics of 60-GHz millimeter waves for ITS inter-vehicle communications," *IEICE Transactions on Communications*, vol. 84, no. 9, pp. 2530–2539, 2001.

[9] S. Takahashi, A. Kato, K. Sato, and M. Fujise, "Distance dependence of path loss for millimeter wave inter-vehicle communications," *Proc. of IEEE Vehicular Technology Conference (VTC-Fall)*, vol. 1, pp. 26–30, 2003.

[10] A. Yamamoto, K. Ogawa, T. Horimatsu, A. Kato, and M. Fujise, "Path-loss prediction models for intervehicle communication at 60 GHz," *IEEE Transactions on Vehicular Technology*, vol. 57, no. 1, pp. 65–78, 2008.

[11] K. Guan, G. Li, T. Kürner, A. F. Molisch, B. Peng, R. He, B. Hui, J. Kim, and Z. Zhong, "On millimeter wave and thz mobile radio channel for smart rail mobility," *IEEE Transactions on Vehicular Technology*, vol. 66, no. 7, pp. 5658–5674, 2017.

[12] V. Va, J. Choi, and R. W. Heath Jr., "The impact of beamwidth on temporal channel variation in vehicular channels and its implications," *IEEE Transactions on Vehicular Technology*, vol. 66, no. 6, pp. 5014–5029, 2017.

[13] J.-J. Park, J. Lee, K.-W. Kim, M.-D. Kim, and K. C. Lee, "28 GHz Doppler measurements in high-speed expressway environments," in *Proc. of IEEE 29th Annual International Symposium on Personal, Indoor and Mobile Radio Communications (PIMRC)*, 2018, pp. 1132–1133.

[14] J. Blumenstein, A. Prokes, J. Vychodil, T. Mikulasek, J. Milos, E. Zöchmann, H. Groll, C. F. Mecklenbräuker, M. Hofer, D. Löschenbrand *et al.*, "Measured high-resolution power-delay profiles of nonstationary vehicular millimeter wave channels," in *Proc. of IEEE 29th Annual International Symposium on Personal, Indoor and Mobile Radio Communications (PIMRC)*, 2018, pp. 1–5.

[15] K.-W. Kim, J.-J. Park, M.-D. Kim, and J. Lee, "Spectral leakage reduction of power-delay-Doppler profile for mm-wave V2I channel," in *2018 International Conference on Information and Communication Technology Convergence (ICTC)*. IEEE, 2018, pp. 346–350.

[16] M. Boban, D. Dupleich, N. Iqbal, J. Luo, C. Schneider, R. Müller, Z. Yu, D. Steer, T. Jamsa, J. Li *et al.*, "Multi-band vehicle-to-vehicle channel characterization in the presence of vehicle blockage," *IEEE Access*, 2019.

[17] A. Prokes, J. Vychodil, T. Mikulasek, J. Blumenstein, E. Zöchmann, H. Groll, C. F. Mecklenbräuker, M. Hofer, D. Löschenbrand, L. Bernadó *et al.*, "Time-domain broadband 60 GHz channel sounder for vehicle-to-vehicle channel measurement," in *Proc. of IEEE Vehicular Networking Conference (VNC)*. IEEE, 2018, pp. 1–7.

[18] E. Zöchmann, C. F. Mecklenbräuker, M. Lerch, S. Pratschner, M. Hofer, D. Löschenbrand, J. Blumenstein, S. Sangodoyin, G. Artner, S. Caban, T. Zemen, A. Prokes, M. Rupp, and A. F. Molisch, "Measured delay and Doppler profiles of overtaking vehicles at 60 GHz," in *Proc. of the 12th European Conference on Antennas and Propagation (EuCAP)*, 2018, pp. 1–5.

[19] H. Groll, E. Zöchmann, S. Pratschner, M. Lerch, D. Schützenhöfer, M. Hofer, J. Blumenstein, S. Sangodoyin, T. Zemen, A. Prokes *et al.*, "Sparsity in the delay-doppler domain for measured 60 ghz vehicle-to-infrastructure communication channels," *arXiv preprint arXiv:1901.10817*, 2019, submitted to ICC 2019.

[20] E. Zöchmann, M. Hofer, M. Lerch, J. Blumenstein, S. Sangodoyin, H. Groll, S. Pratschner, S. Caban, D. Löschenbrand, L. Bernadó, T. Zemen, A. Prokes, M. Rupp, C. F. Mecklenbräuker, and A. F. Molisch, "Statistical evaluation of delay and Doppler spread in 60 GHz vehicle-to-vehicle channels during overtaking," in *Proc. of IEEE-APS Topical Conference on Antennas and Propagation in Wireless Communications (APWC)*, 2018, pp. 1–4.

[21] G. D. Durgin, T. S. Rappaport, and D. A. De Wolf, "New analytical models and probability density functions for fading in wireless communications," *IEEE Transactions on Communications*, vol. 50, no. 6, pp. 1005–1015, 2002.

[22] E. Zöchmann, M. Lerch, S. Pratschner, R. Nissel, S. Caban, and M. Rupp, "Associating spatial information to directional millimeter wave channel measurements," in *Proc. of IEEE Vehicular Technology Conference (VTC-Fall)*, 2017, pp. 1–5.

[23] E. Zöchmann, M. Lerch, S. Caban, R. Langwieser, C. F. Mecklenbräuker, and M. Rupp, "Directional evaluation of receive power, Rician K-factor and RMS delay spread obtained from power measurements of 60 GHz indoor channels," in *Proc. of IEEE-APS Topical Conference on Antennas and Propagation in Wireless Communications (APWC)*, 2016.

[24] E. Zöchmann, K. Guan, and M. Rupp, "Two-ray models in mmWave communications," in *Proc. of Workshop on Signal Processing Advances in Wireless Communications (SPAWC)*, 2017, pp. 1–5.

[25] E. Zöchmann, S. Caban, C. F. Mecklenbräuker, S. Pratschner, M. Lerch, S. Schwarz, and M. Rupp, "Better than Rician: modelling millimetre wave channels as two-wave with diffuse power," *EURASIP Journal on Wireless Communications and Networking*, vol. 2019, no. 1, pp. 1–21, 2019.

[26] E. Zöchmann, M. Hofer, M. Lerch, S. Pratschner, L. Bernadó, J. Blumenstein, S. Caban, S. Sangodoyin, H. Groll, T. Zemen, A. Prokeš, M. Rupp, A. F. Molisch, and C. F. Mecklenbräuker, "Position-specific statistics of 60 GHz vehicular channels during overtaking," *IEEE Access*, vol. 7, pp. 14 216–14 232, 2019.

[27] E. Zöchmann, J. Blumenstein, R. Marsalek, M. Rupp, and K. Guan, "Parsimonious channel models for millimeter wave railway communications," in *Proc. of IEEE Wireless Communications and Networking Conference (WCNC)*, 2019, pp. 1–6.

[28] M. Rao, F. J. Lopez-Martinez, M.-S. Alouini, and A. Goldsmith, "MGF approach to the analysis of generalized two-ray fading models," *IEEE Transactions on Wireless Communications*, vol. 14, no. 5, pp. 2548–2561, 2015.

[29] E. Zöchmann, P. Gerstoft, and C. F. Mecklenbräuker, "Density evolution of sparse source signals," in *Proc. of 3rd International Workshop on Compressed Sensing Theory and its Applications to Radar, Sonar and Remote Sensing (CoSeRa)*. IEEE, 2015, pp. 124–128.

[30] C. F. Mecklenbräuker, P. Gerstoft, and E. Zöchmann, "c–LASSO and its dual for sparse signal estimation from array data," *Signal Processing*, vol. 130, pp. 204–216, 2017.

[31] T. Blazek, E. Zöchmann, and C. F. Mecklenbräuker, "Model order selection for LASSO fitted millimeter wave vehicular channel data," in *Proc. of IEEE 29th Annual International Symposium on Personal, Indoor and Mobile Radio Communications (PIMRC)*. IEEE, 2018, pp. 80–84.

[32] ——, "Approximating clustered millimeter wave vehicular channels by sparse subband fitting," in *Proc. of IEEE 29th Annual International Symposium on Personal, Indoor and Mobile Radio Communications (PIMRC)*. IEEE, 2018, pp. 91–95.

[33] ——, "Millimeter wave vehicular channel emulation: A framework for balancing complexity and accuracy," *Sensors*, vol. 18, no. 11, p. 3997, 2018.